

NASA TN D-7560



(NASA-TN-D-7560) A FILTER SPECTROMETER
CONCEPT FOR FACSIMILE CAMERAS (NASA)
31 p HC \$3.25 CSSL 14E

N74-27874

Unclas
H1/14 42833

A FILTER SPECTROMETER CONCEPT FOR FACSIMILE CAMERAS

*by Daniel J. Jobson, W. Lane Kelly IV,
and Stephen D. Wall*

*Langley Research Center
Hampton, Va. 23665*



1. Report No. NASA TN D-7560	2. Government Accession No.	3. Recipient's Catalog No.	
4. Title and Subtitle A FILTER SPECTROMETER CONCEPT FOR FACSIMILE CAMERAS		5. Report Date June 1974	
		6. Performing Organization Code	
7. Author(s) Daniel J. Jobson, W. Lane Kelly IV, and Stephen D. Wall		8. Performing Organization Report No. L-9356	
		10. Work Unit No. 502-03-52-04	
9. Performing Organization Name and Address NASA Langley Research Center Hampton, Va. 23665		11. Contract or Grant No.	
		13. Type of Report and Period Covered Technical Note	
12. Sponsoring Agency Name and Address National Aeronautics and Space Administration Washington, D.C. 20546		14. Sponsoring Agency Code	
		15. Supplementary Notes	
16. Abstract A concept which utilizes interference filters and photodetector arrays to integrate spectrometry with the basic imagery function of a facsimile camera is described and analyzed. The analysis considers spectral resolution, instantaneous field of view, spectral range, and signal-to-noise ratio. Specific performance predictions for the Martian environment, the Viking facsimile camera design parameters, and a signal-to-noise ratio for each spectral band equal to or greater than 256 indicate the feasibility of obtaining a spectral resolution of 0.01 μm with an instantaneous field of view of about 0.1° in the 0.425- to 1.025- μm range using silicon photodetectors and a spectral resolution of 0.05 μm with an instantaneous field of view of about 0.6° in the 1.0- to 2.7- μm range using lead sulfide photodetectors.			
17. Key Words (Suggested by Author(s)) Planetary lander instrumentation Spectrometry Facsimile cameras		18. Distribution Statement Unclassified - Unlimited STAR Category 14	
19. Security Classif. (of this report) Unclassified	20. Security Classif. (of this page) Unclassified	21. No. of Pages 29	22. Price* \$3.25

A FILTER SPECTROMETER CONCEPT FOR FACSIMILE CAMERAS

By Daniel J. Jobson, W. Lane Kelly IV, and Stephen D. Wall
Langley Research Center

SUMMARY

A concept which utilizes interference filters and photodetector arrays to integrate spectrometry with the basic imagery function of a facsimile camera is described and analyzed. The analysis considers spectral resolution, instantaneous field of view, spectral range, and signal-to-noise ratio. Specific performance predictions for the Martian environment, the Viking facsimile camera design parameters, and a signal-to-noise ratio for each spectral band equal to or greater than 256 indicate the feasibility of obtaining a spectral resolution of $0.01 \mu\text{m}$ with an instantaneous field of view of about 0.1° in the $0.425\text{-}1.025\text{-}\mu\text{m}$ range using silicon photodetectors and a spectral resolution of $0.05 \mu\text{m}$ with an instantaneous field of view of about 0.6° in the $1.0\text{-}2.7\text{-}\mu\text{m}$ range using lead sulfide photodetectors.

INTRODUCTION

Imagery from flyby, orbiter, and lander spacecraft provides important information about the planet's structure, active processes, and (to a much lesser extent) composition. Further data on composition from flybys and orbiters are generally provided by optical spectrometers and from landers by direct molecular analyses. Nonetheless, spectrometric measurements from a lander could provide valuable data on surface composition beyond the reach of a soil sampler and could provide a spectral link between local lander investigations and planet-wide orbiter investigations in the same way as the lander imaging system provides a spatial link. Spectrometric measurements from a roving vehicle could also aid in locating features of scientific interest for further investigation. Finally, optical spectrometer techniques may prove particularly valuable for lander missions which cannot support the weight and complexity of equipment required for direct molecular analysis.

The facsimile camera is an attractive candidate as an imaging device for planetary landers and has been selected for the Viking missions for Mars because of its small size, low weight, and low power requirements. Other advantages are that it can provide accurate radiometric and photogrammetric data because a single photodetector scans a complete

field of view and can provide buffer-free operation because scan rates can be synchronized with low data transmission rates. In addition to spatially characterizing a scene, this device also has the potential capability to provide spectral characterization.

This paper introduces a concept which utilizes interference filters and photodetector arrays to achieve a spectrometry capability without adding significant optical or mechanical complexity to the facsimile camera or interfering with its imagery function. A first-order performance analysis of this concept is presented to predict its potential spectral and spatial resolution, spectral range, and signal-to-noise ratio. Pertinent Martian environment data and Viking lander camera characteristics are used to demonstrate the feasibility of implementing this concept.

SYMBOLS

A	photodetector active area, cm^2
D	objective aperture diameter, cm
D_{λ}^*	spectral detectivity of photodetector, $\text{cm-Hz}^{1/2}/\text{W}$
d	diameter of the on-axis photodetector element, cm
f	focal length of camera optics, cm
k	number of photodetector elements in an array
L	dummy variable for range of in-focus object distance, cm
L_f	far distance of depth of field, cm
L_n	near distance of depth of field, cm
L_o	in-focus object distance from camera optics, cm
ΔL	depth of field, cm
l	dummy variable for range of in-focus image distance, cm
l_f	image plane distance from camera optics in focus for object distance L_f , cm (see fig. 4(c))

l_n	image plane distance from camera optics in focus for object distance L_n , cm (see fig. 4(b))
l_o	distance from camera optics to on-axis photodetector aperture, cm
l'_o	distance from camera optics to off-axis photodetector aperture, cm
Δl	depth of focus, cm
n	number of repetitive samples per spectral band
S/N	ratio of signal to rms noise
S_λ	solar spectral irradiance above a planetary atmosphere, $W/cm^2-\mu m$
s	distance from mirror rotation axis to principal point of the optics, cm
W	electronic bandwidth, hertz
y	position of a picture element assuming mirror rotation axis is on the principal point of the optics
y'	position of a picture element assuming mirror rotation axis is separated from the principal point of the optics by a distance s
α	angular subtense of edge-to-edge photodetector spacing, deg or rad
β	instantaneous field of view, deg or rad
β_c	constant instantaneous field of view, deg or rad
ϵ	angle determining position of picture element (see fig. 2)
θ	angle of a photodetector element from the optical axis, deg or rad
θ_A	half-angle of image field subtended by photodetector array, rad or deg
θ'_A	half-angle of image field subtended by photodetector array assuming $\alpha = \frac{\beta_c}{2}$, rad or deg

λ	wavelength, μm
λ'	center wavelength of interference filter, μm
λ_1	lower limit of spectral range, μm
λ_2	upper limit of spectral range, μm
$\Delta\lambda$	spectral bandwidth of an ideal square band-pass interference filter, μm
ρ_λ	average albedo of planetary surface
τ_F	transmissivity of ideal square band-pass interference filter
τ_λ	spectral transmissivity of planetary atmosphere
$\tau_{\lambda,f}$	spectral transmissivity of interference filter
$\tau_{\lambda,l}$	spectral transmissivity of camera optics
ϕ	illumination scattering function of planetary surface

DESCRIPTION OF CONCEPT

A basic configuration of the facsimile camera as an imager is shown in figure 1(a). Figure 1(b) shows the same mechanical structure and optics arranged for spectrometric measurements. Radiation from the scene is reflected by the scanning mirror, captured by the objective optics, and projected onto a plane which contains either a single detector (fig. 1(a)) or an array of interference filters and photodetectors (fig. 1(b)).

For the imaging mode, the output of a photodetector is monitored continuously as the scan mirror moves the image across the plane containing the photodetector. This image motion permits the photodetector to scan a vertical strip of the scene. The camera is rotated slowly in azimuth so that an entire scene is imaged as a sequence of vertical lines. As a result of this process, the spatial distribution of radiance levels is measured while the wavelength range of the measurement is held constant.

By contrast, the spectrometer mode of operation holds the spatial position constant while varying the wavelength range of the measurement as the mirror rotates. The spatial position is held constant by the use of tracking electronics which sequence down the detector array synchronous with image motion. Wavelength variation is provided by interference filters mounted over the photodetector elements.

The integration of the imaging and spectrometry functions within a facsimile camera is accomplished by incorporating both the imaging detector and the spectrometry array with their associated electronics into a single instrument. A major conflict in requirements for the two functions occurs when the objective optics aperture size is chosen. Since the imaging function requires a large depth of field, a small aperture is necessary for this mode. In contrast, the spectrometry mode requires more energy and therefore a larger aperture. For this analysis, the aperture size is chosen to fit the imaging function requirements, since the imaging function is the more basic one. The disadvantage of using the small aperture for the spectrometry function is compensated for by (1) repeated sampling of the same line, (2) increasing the picture element size, and (3) decreased electronic bandwidth.

A performance analysis of the imagery mode is presented in reference 1 and will not be repeated here. In that analysis, the important performance parameters were instantaneous field of view, signal-to-noise ratio, depth of field, and scanning rate. It was found that these parameters were so closely interrelated that any improvement in one could be accomplished only at the expense of others, or at the expense of design simplicity.

For the spectrometry mode, the most important performance parameters are spectral resolution, spectral range, instantaneous field of view, and signal-to-noise ratio. In addition, the total image field required by the photodetector array leads to important optics design requirements.

ANALYSIS OF THE SPECTROMETRY MODE

While the analysis of the facsimile camera imagery mode in reference 1 was concerned with a single broad spectral band (the spectral range of the photodetector) and on-axis optics, the spectrometry mode is concerned with narrow spectral bandwidths ranging over the spectral response of the photodetectors and off-axis optics. As a result, the spectroradiometric and optical performance of the spectrometer concept must be investigated.

Spectroradiometric Performance Parameters

The basic equation which governs the electro-optical performance of the facsimile camera is given by reference 1 as

$$\frac{S}{N} = \frac{\pi\beta^2 D^2 \phi}{16 \left(A \frac{W}{h}\right)^{1/2}} \int_0^\infty S_\lambda \tau_\lambda \rho_\lambda \tau_{\lambda, l} \tau_{\lambda, f} D_\lambda^* d\lambda \quad (1)$$

The major performance parameters for the spectrometry mode are the ratio of signal to rms noise S/N , instantaneous field of view β (in radians), spectral resolution

determined by the shape of the filter transmissivity curve $\tau_{\lambda,f}$, and total spectral range which is determined by the remaining parameters in the integral.

The camera design parameters are the optics aperture diameter D , the transmissivity of the optics $\tau_{\lambda,l}$, the photodetector spectral detectivity D_{λ}^* , the photodetector active area A , the electronic bandwidth W , and the number of samples per picture element in each spectral band n .

The environmental parameters are the surface illumination scattering function ϕ (a function of lighting and viewing geometry), the albedo ρ_{λ} , the solar spectral irradiance S_{λ} , and the atmospheric transmissivity τ_{λ} .

Since the evaluation of equation (1) is of interest only for narrow spectral bandwidths, the wavelength integration is not required for a first-order analysis. Consequently, the spectral transmissivity $\tau_{\lambda,f}$ of the filter may be approximated by an ideal square band-pass with a constant transmissivity value τ_F and spectral bandwidth $\Delta\lambda$. Using these approximations, equation (1) can be rewritten as

$$\left(\frac{S/N}{\Delta\lambda} \beta^2\right)_{\lambda'} = \frac{\pi D^2 \tau_F \phi}{16 \left(A \frac{W}{n}\right)^{1/2}} S_{\lambda'} \tau_{\lambda'} \rho_{\lambda'} \tau_{\lambda'} l D_{\lambda'}^* \quad (2)$$

where λ' is the center wavelength of the spectral filter. The performance parameters of special interest are grouped on the left side of the equation.

Optical Analysis

In order to properly track the moving image of the scene down the spectrometer array, it is necessary to establish the relationship between a given mirror angle and the position of the image of a certain picture element in the scene. In addition, the instantaneous field of view must be considered, along with the total angular image field required by the photodetector array and the allowable depth of focus. Finally, the impact of those values on the imaging optics must be considered.

Position of a picture element. - If the axis of rotation of the mirror coincided with both nodal points of the optics, then the position of a picture element would be given by

$$y = l_0 \tan \theta \quad (3)$$

where θ is twice the angle of rotation of the mirror and $y = 0$ ($\theta = 0^\circ$) corresponds to an on-axis ray. (See fig. 2.)

However, since the axis of rotation of the mirror is displaced a distance from the first nodal point of the optics, the position of a picture element becomes

$$y' = s \tan \theta + l_0 \tan \epsilon \quad (4a)$$

Since

$$\tan \epsilon = \frac{(f - s)\tan \theta}{f}$$

equation (4a) can also be written as

$$y' = \left[s + \frac{l_0(f - s)}{f} \right] \tan \theta \quad (4b)$$

The error incurred by assuming the mirror axis and both nodal points of the optics to be identical is then

$$\Delta y = y - y' = \frac{s}{f}(l_0 - f)\tan \theta \quad (5)$$

This error can be minimized, if it is sizable, by designing the photodetector element positions according to equation (4b).

Instantaneous field of view.- The instantaneous field of view for an on-axis photodetector element is given by

$$\beta = 2 \tan^{-1} \frac{d}{2l_0} \quad (6)$$

For a detector at an arbitrary off-axis point (fig. 3) the instantaneous field of view becomes

$$\beta = 2 \tan^{-1} \frac{d \cos \theta}{2l_0/\cos \theta} \quad (\text{for } d \ll 2l_0) \quad (7a)$$

$$\beta = \frac{d \cos^2 \theta}{l_0} \quad (\text{for small } \beta) \quad (7b)$$

To avoid variations in instantaneous field of view, which in turn result in variations in spectral data not directly proportional to scene spectral reflectance, a constant instantaneous field of view can be obtained by varying the aperture diameters of photodetector elements so that

$$\beta_c = \frac{d(\theta)\cos^2 \theta}{l_0} \quad (8)$$

where

$$d(\theta) = \frac{d}{\cos^2 \theta}$$

so that

$$\beta_c = \frac{d}{l_0}$$

Otherwise, the resulting signal variations with spatial rather than spectral origin must be taken into account.

The angular spacing (edge to edge) of detector elements α also possesses a $\cos^2\theta$ dependency which can be corrected if necessary by varying the spacing between photodetector elements or by properly controlling the sampling intervals by an electronic function generator.

Angular image field.- The angular image field required by the spectrometer photodetector array is expressed here as a function of constant instantaneous field of view, spectral bandwidth, and spectral range. From figure 3, the half-angle θ_A of the required image field may be written as

$$\theta_A = \frac{1}{2} [k\beta_c + (k - 1)\alpha] \quad (9a)$$

where the angular subtense α of the edge-to-edge detector spacing is assumed constant and the number of spectral channels (filtered detectors) k equals $\frac{\lambda_2 - \lambda_1}{\Delta\lambda}$ rounded to an integer.

For this analysis a constant angular subtense $\alpha = \frac{\beta_c}{2}$ is chosen as an example so that equation (9a) becomes

$$\theta'_A = \frac{1}{4}(3k - 1)\beta_c \quad (9b)$$

Depth of focus.- When an object in the scene is in focus for the photodetector array, then the picture element, defined by the instantaneous field of view β , has an unambiguous meaning since all the light emitted from this area and captured by the optics is also, according to first-order geometrical optics, incident on the detector aperture. However, as soon as the picture element is no longer in focus, its meaning becomes ambiguous since not all the light emitted from this area and captured by the optics is incident on the detector aperture and some light not emitted from this area is incident on the detector aperture. Ranges of distances over which defocus degradation is generally acceptable are illustrated in figure 4(a) and are called the depth of focus of the image field and depth of field on the object field. From the geometry shown in figure 4(a), the on-axis range of acceptable focus in image space may be expressed as

$$l_f \leq l \leq l_n \quad (10a)$$

or

$$\frac{l_o}{1 + \frac{\beta l_o}{D}} \leq l \leq \frac{l_o}{1 - \frac{\beta l_o}{D}} \quad (10b)$$

The corresponding range of acceptable focus in object space is

$$L_n \leq L \leq L_f \quad (11a)$$

or

$$\frac{D/\beta}{\frac{D}{\beta L_o} + 1} \leq L \leq \frac{D/\beta}{\frac{D}{\beta L_o} - 1} \quad (11b)$$

where $\frac{1}{f} = \frac{1}{L_o} + \frac{1}{l_o}$, and f is the focal length of the lens.

The off-axis depth of focus (figs. 4(b) and 4(c)) reduces to the same form as equation (10b). However, if β is kept constant off-axis for photodetectors by varying d according to equation (8), then the range of acceptable focus for image space is given by

$$\frac{l_o}{1 + \frac{\beta_c l_o}{D \cos^2 \theta}} \leq l \leq \frac{l_o}{1 - \frac{\beta_c l_o}{D \cos^2 \theta}} \quad (12)$$

The corresponding range of acceptable focus for object space is

$$\frac{\frac{D \cos^2 \theta}{\beta_c}}{\frac{D \cos^2 \theta}{\beta_c L_o} + 1} \leq L \leq \frac{\frac{D \cos^2 \theta}{\beta_c}}{\frac{D \cos^2 \theta}{\beta_c L_o} - 1} \quad (13)$$

PERFORMANCE TRADE-OFF ANALYSIS

Certain assumptions were made in using equation (2) to analyze the spectroradiometric performance of the spectrometer concept. Results of the foregoing analysis are now used to evaluate the potential performance capability of the spectrometer concept as applied to a mission to Mars. Emphasis is placed on the major performance parameters – spectral resolution, spectral range, instantaneous field of view, and signal-to-noise ratio – but optical design parameters such as angular image field and depth of focus are also considered.

Assumptions and Constraints

Pertinent properties on the Martian environment (fig. 5) are taken from a "Mars Engineering Model" for the 0.3- to 1.1- μ m wavelength range. For the 1.1- to 3.0- μ m range, solar spectral irradiance data are taken from reference 2 and adjusted for the

1.52 astronomical unit mean distance of Mars from the Sun, and the atmospheric transmissivity and surface albedo are extrapolated as constants from their $1.1\text{-}\mu\text{m}$ values taken from a "Mars Engineering Model." This extrapolation was necessary because of the lack of accepted engineering data.

This analysis will be restricted to the existing optical design parameters of the Viking lander camera since the spectrometry mode must be compatible with an imagery mode and must utilize the same optics. It is assumed, however, that the optics are capable of transmitting radiation out to $3.0\ \mu\text{m}$. This can be accomplished by the use of reflecting optics or an appropriate infrared transmitting lens material.

The photodetectors considered here are silicon (Si) and lead sulfide (PbS). The spectral detectivity of these photodetectors is shown in figure 6. The value of W/n in equation (2) is assumed to be unity since the number of samples per spectral band n can be used to compensate for the electronic bandwidth W imposed on the spectrometer by the imaging system. For example, the bandwidth for the slow scan rate of the Viking facsimile camera is 25 Hz; therefore, 25 samples per spectral band can be used to achieve $\frac{W}{n} = 1$. All other assumptions are included in table I.

Results

Spectroradiometric performance.- The variation of signal-to-noise ratio with wavelength is given for various values of instantaneous field of view and spectral bandwidth in figure 7 for Si and in figure 8 for PbS. From these curves, it is observed that minimum signal-to-noise ratio occurs at the upper and lower extremes of wavelength for Si and at the upper extreme of wavelength limit for PbS. Of particular importance is the upper wavelength limit of the Si detector for overlap with the PbS detector spectral range and the lower limit of Si and upper limit of PbS for the total spectral range.

Using $\frac{S}{N} = 256$ as minimum acceptable signal-to-noise ratio (64 detectable digital encoding levels), the trade-off between instantaneous field of view and spectral bandwidth is examined in figure 9 at $\lambda = 0.900, 0.950, 1.000, 1.025, 1.050,$ and $1.075\ \mu\text{m}$ for Si and at $\lambda = 2.5, 2.6, 2.7, 2.8, 2.9,$ and $3.0\ \mu\text{m}$ for PbS. The lower wavelength limit of Si is then determined by the selection of the upper wavelength limit by using figure 7(a).

The curves in figure 9 indicate a lower limit on spectral bandwidth as a function of the instantaneous field of view. For Si and PbS, respectively, these limits are about $0.01\ \mu\text{m}$ and $0.05\ \mu\text{m}$ for the selected signal-to-noise criterion and reasonable values of spectral range. For cases other than these specific ones, instantaneous field of view can be traded for improved spectral resolution, but only up to the point where large sacrifices in instantaneous field of view yield slight improvement in spectral resolution.

The selection of spectral range limits is based on figure 10. These results show no sharp cutoff with increasing $\beta\Delta\lambda$. Although the information in figure 10 does not define the actual wavelength limits of the spectral range, it illustrates the diminishing returns of continually increasing $\beta\Delta\lambda$.

A specific case is now examined for both Si and PbS. Using figure 9(a), for $\lambda' > 1.025 \mu\text{m}$, the $\beta\Delta\lambda$ curves are more widely spaced so that significantly higher $\beta\Delta\lambda$ values would be required. Also $\lambda' = 1.025 \mu\text{m}$ is a good choice for the overlap point between Si and PbS spectral ranges (see fig. 6). For this choice of λ' , it is noted from figure 9(a) that below $\Delta\lambda = 0.01 \mu\text{m}$, much larger values of β are required to maintain the minimum signal-to-noise ratio. Therefore, $\Delta\lambda = 0.01 \mu\text{m}$ is chosen for Si and a $\beta = 0.12^\circ$ is required. From figure 10, $\lambda_2 - \lambda_1 = 0.6 \mu\text{m}$ resulting in a lower limit on wavelength λ_1 of $0.425 \mu\text{m}$.

For the PbS case, figure 9(b) is used to select $\lambda' = 2.7 \mu\text{m}$. Although the $\beta\Delta\lambda$ curves become widely spaced for $\lambda' > 2.8 \mu\text{m}$, $\lambda' = 2.7 \mu\text{m}$ is selected as a more conservative value to minimize $\beta\Delta\lambda$ because of the lack of Mars engineering data in the PbS spectral range and the difficult optical design requirements which result from large values of β . For $\lambda' = 2.7 \mu\text{m}$ and $\Delta\lambda < 0.05 \mu\text{m}$, large increases in β are required. Therefore, $\Delta\lambda = 0.05 \mu\text{m}$ is selected for spectral bandwidth and $\beta = 0.63^\circ$ is necessary for minimum signal-to-noise ratio. From figure 10, $\lambda_2 - \lambda_1 = 1.7 \mu\text{m}$ resulting in a lower limit on wavelength λ_1 of $1.0 \mu\text{m}$.

Optical design considerations.- After spectral, spatial, and radiometric requirements are established for the spectrometer, their impact on the optics' requirements must be examined, since both a wide image field and a wide spectral range are required.

The position of the picture element, depth of focus, and angular image field requirement can be calculated. Of these three, the angular image field is the most important since the photodetector elements can be spaced to coincide with the position of the picture element and depth of focus is usually greater than depth of focus for the camera's imaging function due to larger values of instantaneous field of view.

No attempt will be made here to trade off the optical design considerations, but there are several approaches which could be taken. The most obvious is to use reflecting optics and to force a large image field with aspheric mirrors. Chromatic aberration would be zero, and the primary spectrally independent aberrations introduced could be tolerated because of the large instantaneous field of view.

An alternate approach would be to ignore the field curvature and balance chromatic aberration with refracting optics and to tilt the photodetector array to bring it into acceptable focus. At any rate the design problem is solvable, if difficult, and, as long as θ_A does not exceed about 25° , the difficulty is not extreme.

Figure 11 shows the half-angle of total image field θ'_A as a function of instantaneous field of view for $\frac{S}{N} = 256$ at the spectral ranges of 0.425 to 1.025 μm for Si and 1.0 to 2.7 μm for PbS. The half-angle of total image field increases approximately as a function of β^2 for the minimum signal-to-noise ratio case. For the previous examples ($\Delta\lambda = 0.01 \mu\text{m}$, $\lambda_2 - \lambda_1 = 1.025 - 0.425 \mu\text{m}$, and $\beta = 0.12^\circ$ for Si; and $\Delta\lambda = 0.05 \mu\text{m}$, $\lambda_2 - \lambda_1 = 2.7 - 1.0 \mu\text{m}$, and $\beta = 0.63^\circ$ for PbS), the half-angles of image field are 5.4° and 16° , respectively.

CONCLUDING REMARKS

A filter spectrometer concept for the facsimile camera was described. This concept neither interferes with the existing imagery function of the facsimile camera nor adds significant optical or mechanical complexity. Since the spectrometer concept utilizes the imaging optics of the facsimile camera, the performance of this spectrometer is generally restricted by the limited objective aperture dictated by the depth of field requirements of the imaging function.

Analysis of spectral resolution, instantaneous field of view, spectral range, and signal-to-noise ratio revealed that for a minimum acceptable ratio of signal to noise in each spectral band and for a fixed spectral range, spectral resolution and instantaneous field of view are inversely related and may be traded against each other. Because of the nature of this relationship, there exists a limit on spectral resolution which is reached when a significant sacrifice in spatial resolution produces only a small improvement in spectral resolution. In contrast to the other performance parameters which are closely interrelated, spectral range depends primarily on the transmission of the optics and photosensor detectivity characteristics.

Using the Martian environment and the optical design parameters of the Viking lander camera as a specific example, a preliminary trade-off analysis was made between the major spectrometer performance parameters. It was found that for a ratio of signal to rms noise of 256, a spectral range extending from 0.425 to 2.7 μm can be covered using silicon photodetectors below 1.025 μm and lead sulfide photodetectors above that wavelength. Spectral bandwidths of 0.01 μm (60 spectral channels) for the silicon range and of 0.05 μm (34 spectral channels) for the lead sulfide range could be obtained with instantaneous fields of view of 0.12° and 0.63° , respectively. The silicon photodetector array subtends a 10.8° total image field while the lead sulfide array subtends a 32° total image field.

Langley Research Center,
National Aeronautics and Space Administration,
Hampton, Va., February 27, 1974.

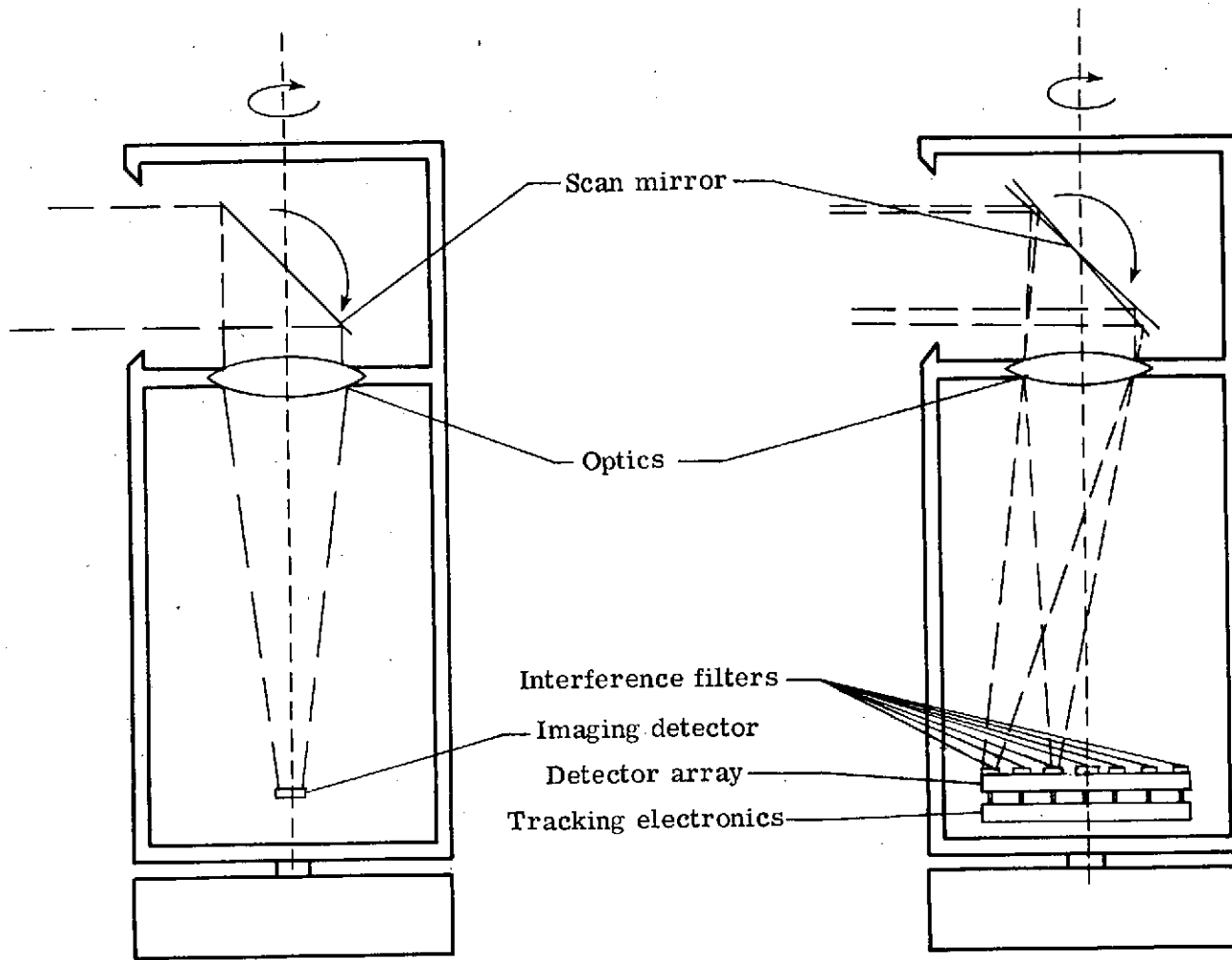
REFERENCES

1. Huck, Friedrich O.; and Lambiotte, Jules J., Jr.: A Performance Analysis of the Optical-Mechanical Scanner as an Imaging System for Planetary Landers. NASA TN D-5552, 1969.
2. Moon, Parry: Proposed Standard Solar-Radiation Curves for Engineering Use. J. Franklin Inst., vol. 230, no. 5, Nov. 1940, pp. 583-617.

TABLE I.- ASSUMPTIONS FOR PERFORMANCE TRADE-OFF ANALYSIS

[Values for eq. (2)]

Objective aperture diameter, D , cm	1.0
Filter transmissivity, τ_F	0.5
Illumination scattering function, ϕ	1
Photodetector active area, A	$\pi\beta^2 l_0^2/4$
Distance from camera optics to on-axis photodetector aperture, l_0 , cm	5.4
Ratio of electronic bandwidth to number of repetitive samples, W/n	1
Solar spectral irradiance above Martian atmosphere, S_λ	Figure 5(a)
Transmissivity of Martian atmosphere, τ_λ	Figure 5(b)
Average albedo of Martian surface, ρ_λ	Figure 5(c)
Transmissivity of camera optics, $\tau_{\lambda,l}$	0.9
Detectivity of photodetector element, D_λ^*	Figure 6



(a) Imager.

(b) Spectrometer.

Figure 1.- A basic configuration of the facsimile camera as an imager and a spectrometer.

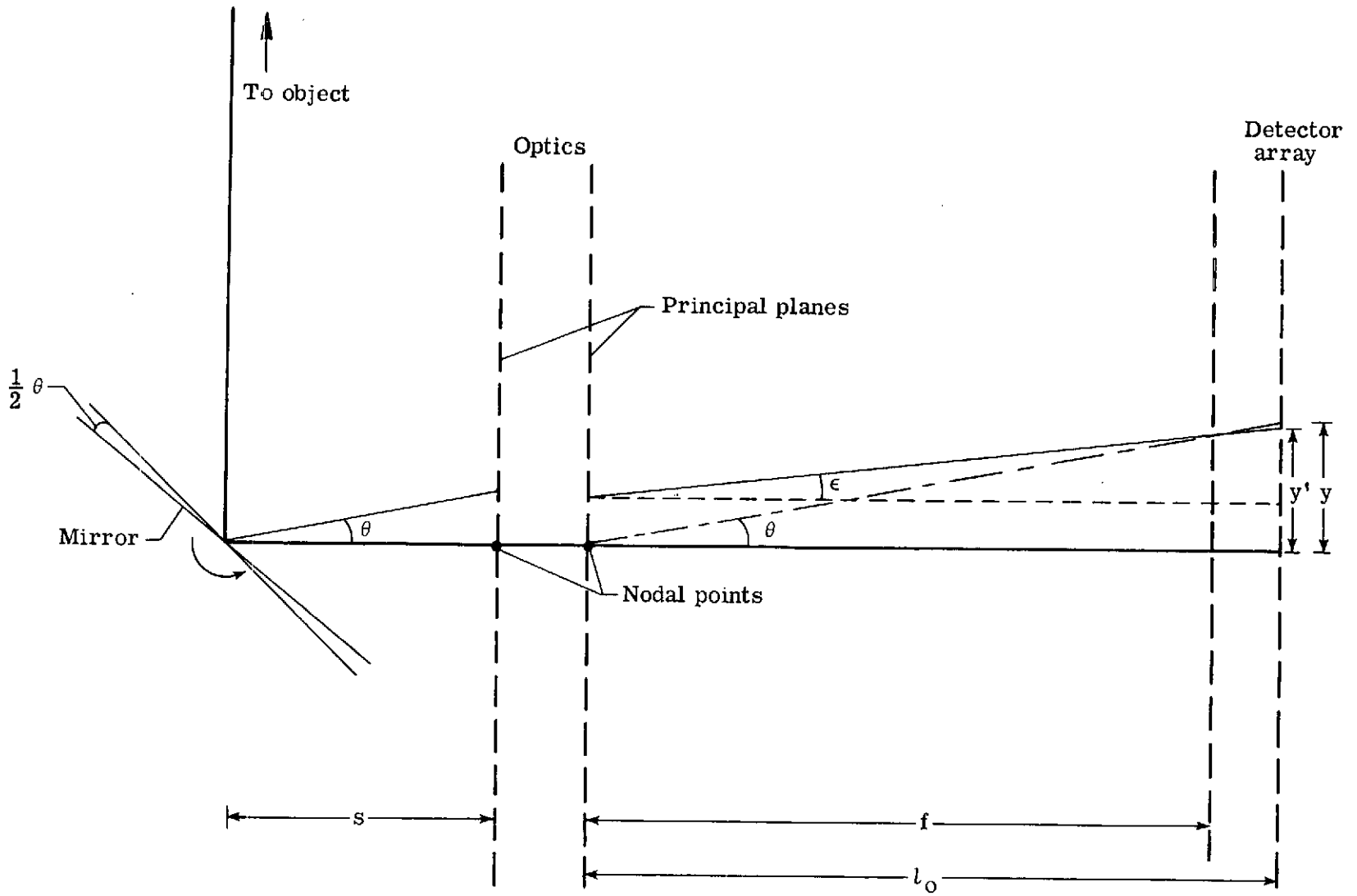
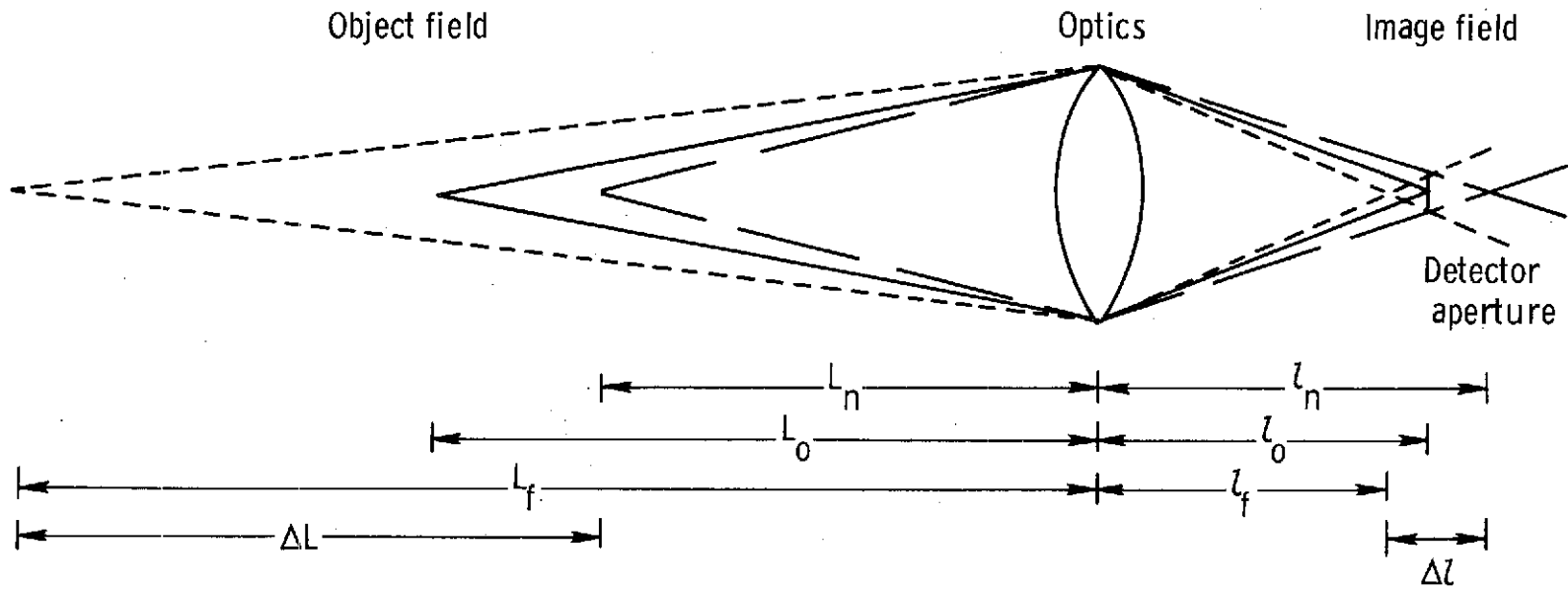
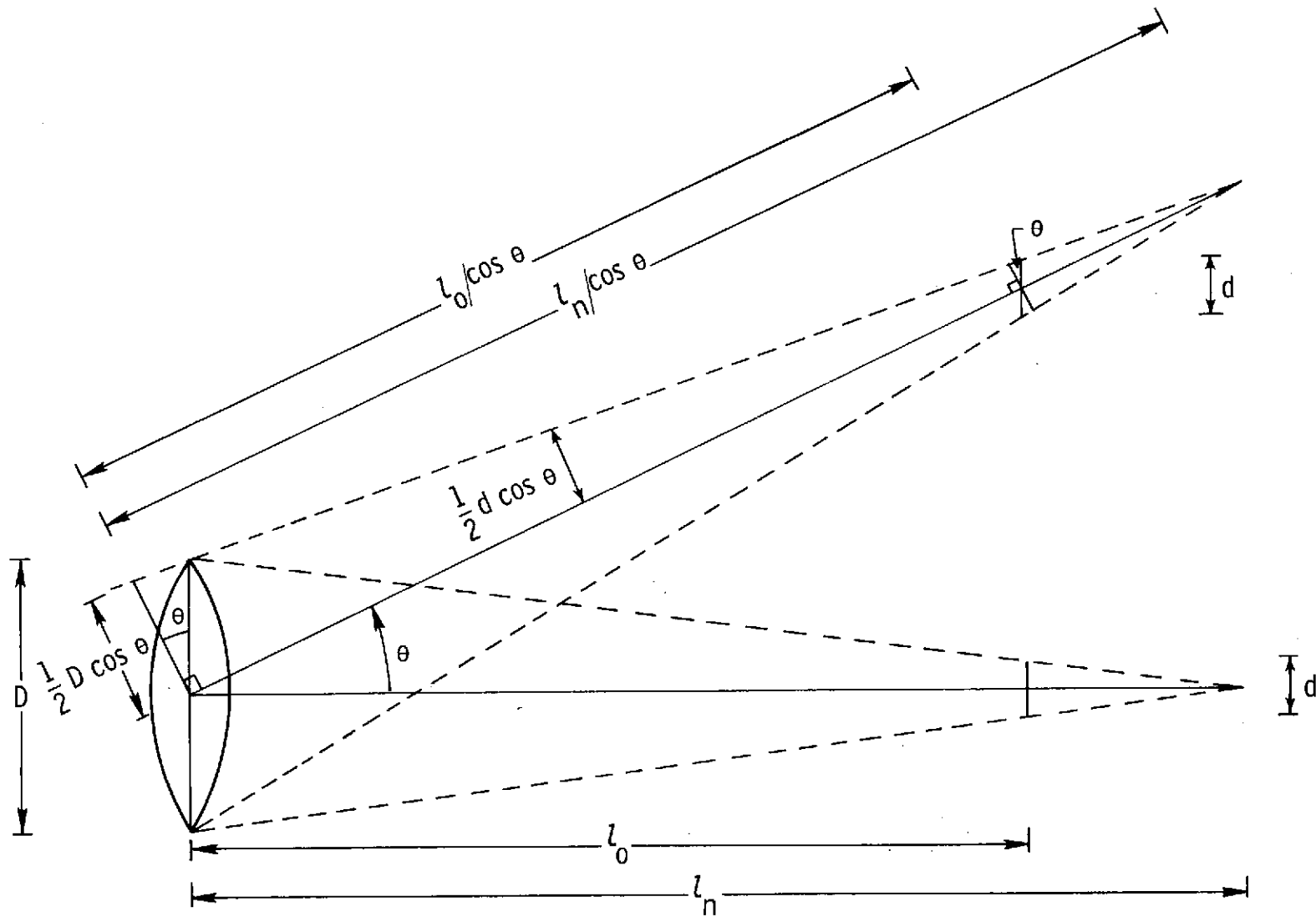


Figure 2.- Geometry for the position of a picture element.



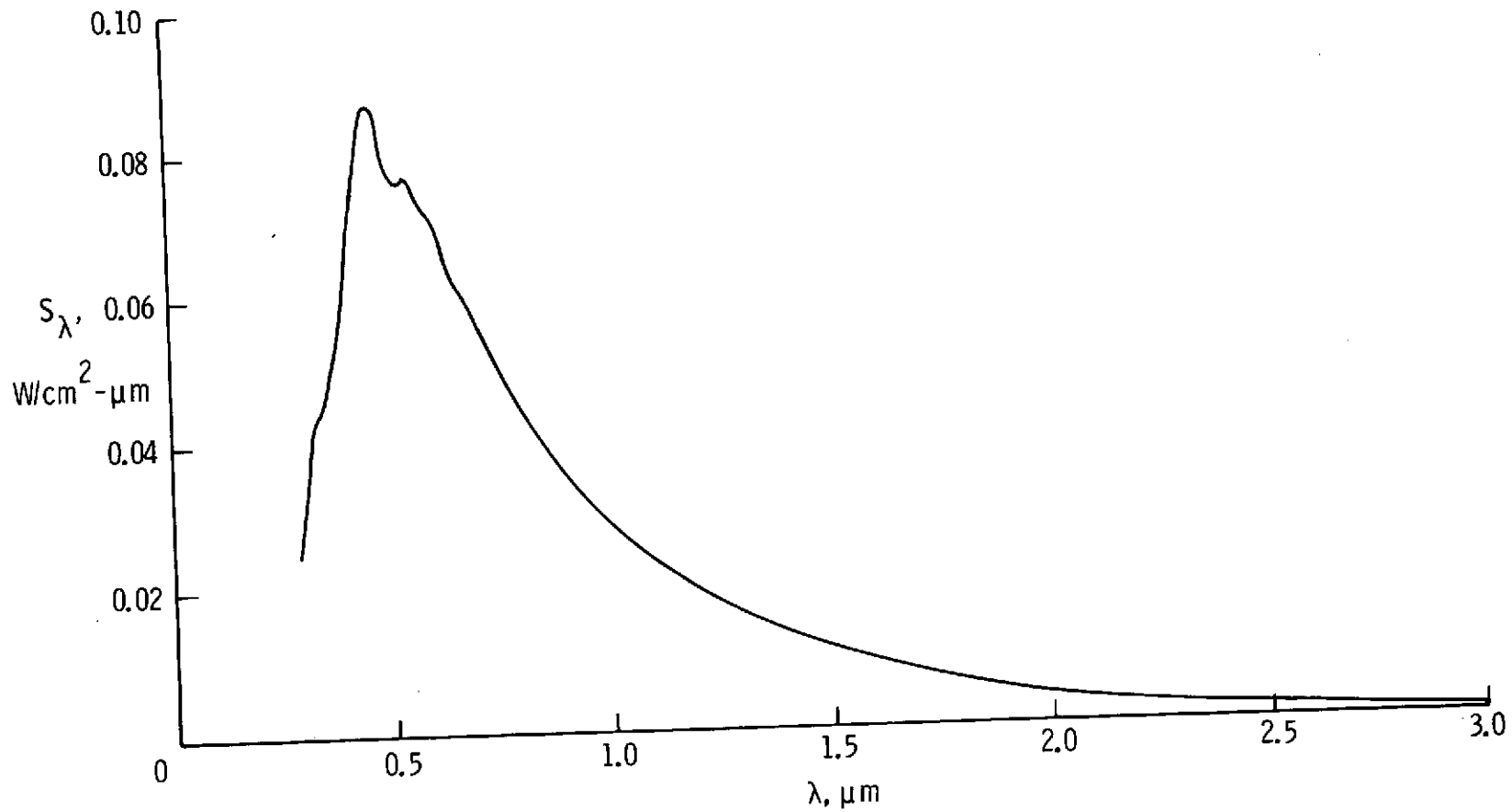
(a) On-axis depth of field and depth of focus.

Figure 4.- Focus geometry.



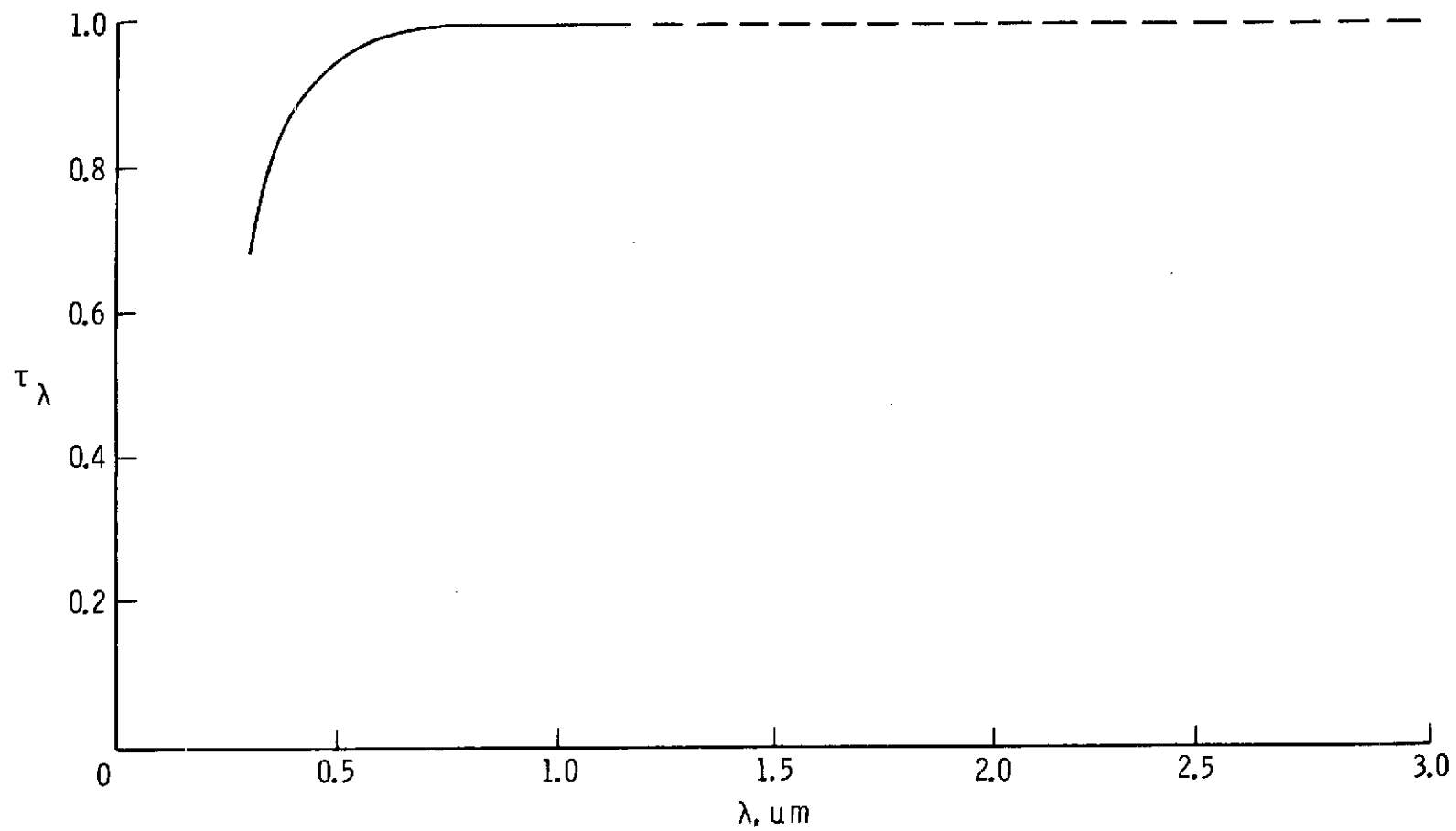
(b) Image field for nearest in-focus object field.

Figure 4. - Continued.



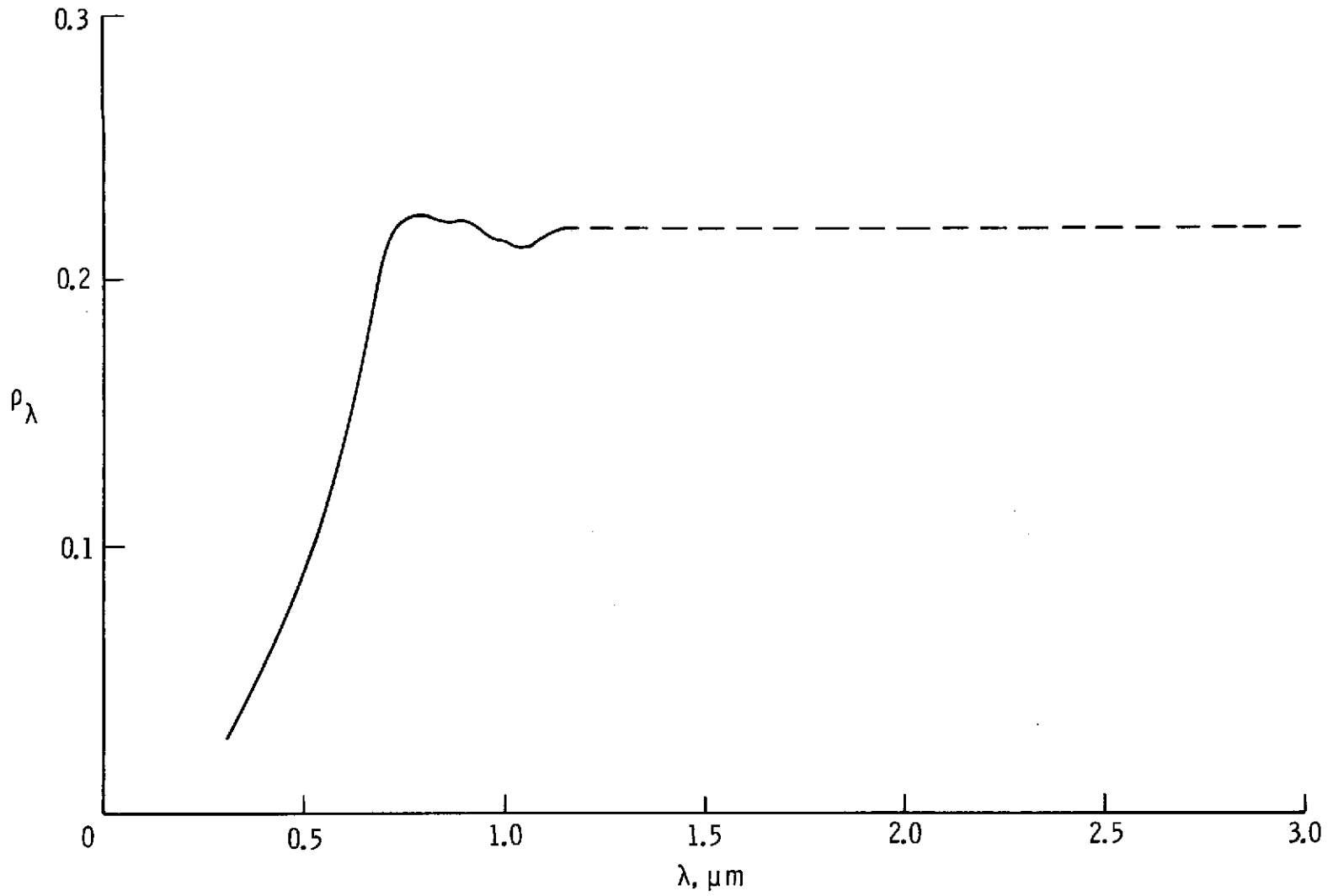
(a) Solar irradiance at 1.52 AU.

Figure 5.- Properties of Martian environment.



(b) Spectral transmissivity of atmosphere.

Figure 5.- Continued.



(c) Average albedo of surface.

Figure 5.- Concluded.

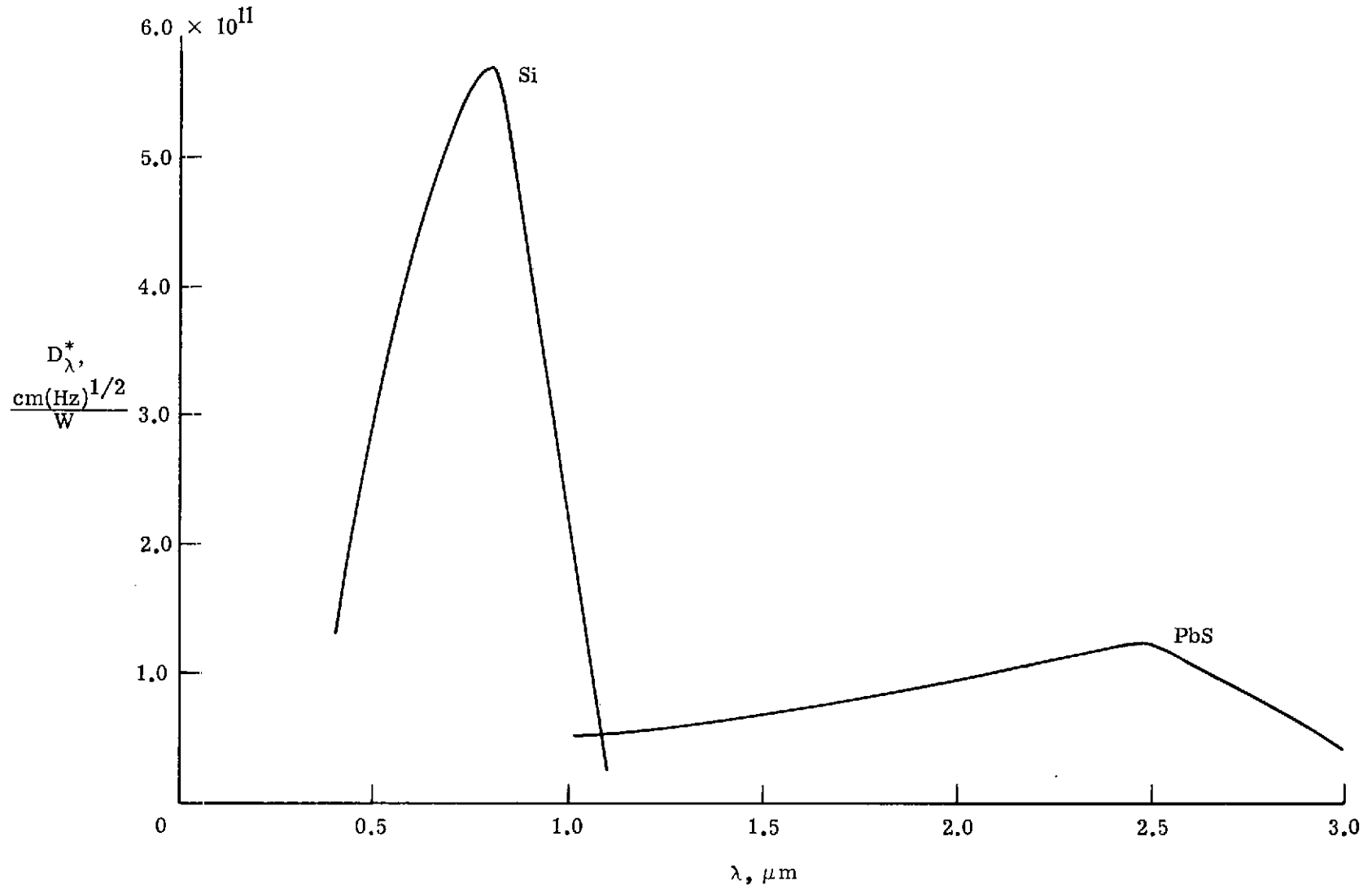
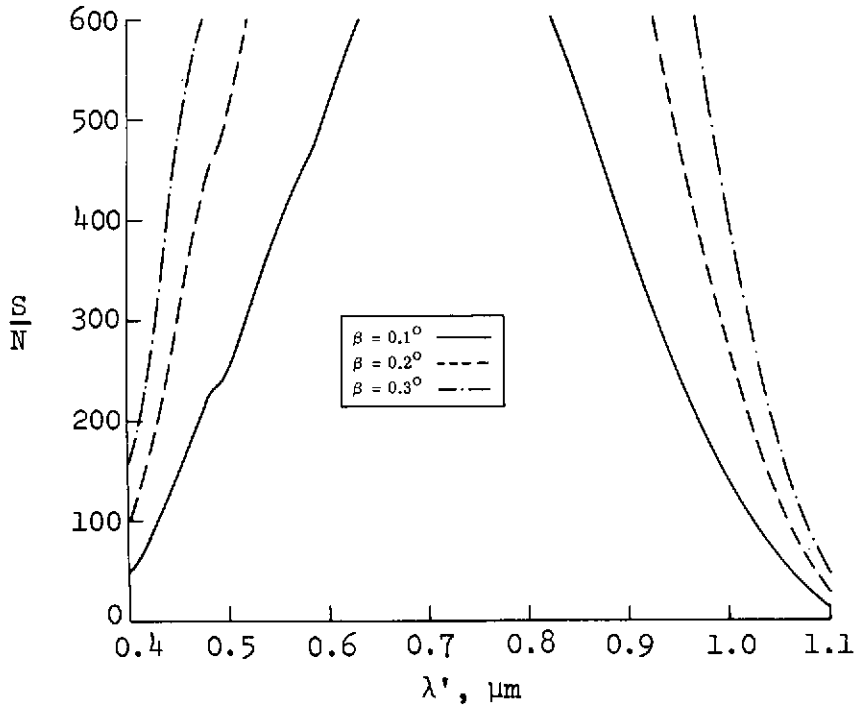
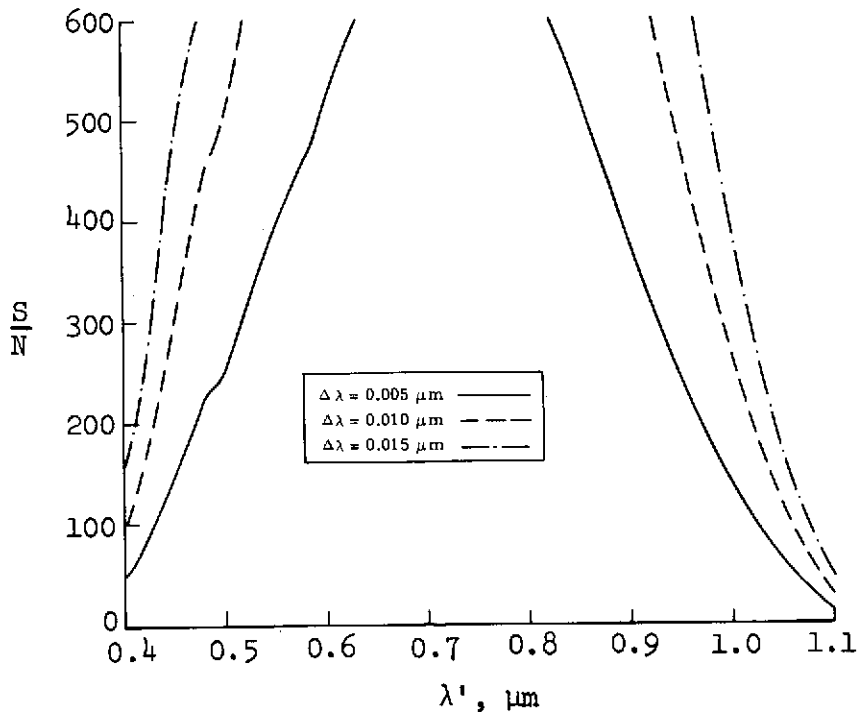


Figure 6.- Spectral detectivities of photodetectors.



(a) $\Delta\lambda = 0.005 \mu\text{m}$.



(b) $\beta = 0.1^\circ$.

Figure 7.- Ratio of signal to rms noise for silicon photodetector as a function of the filter center wavelength for constant (a) spectral resolution and (b) instantaneous field of view.

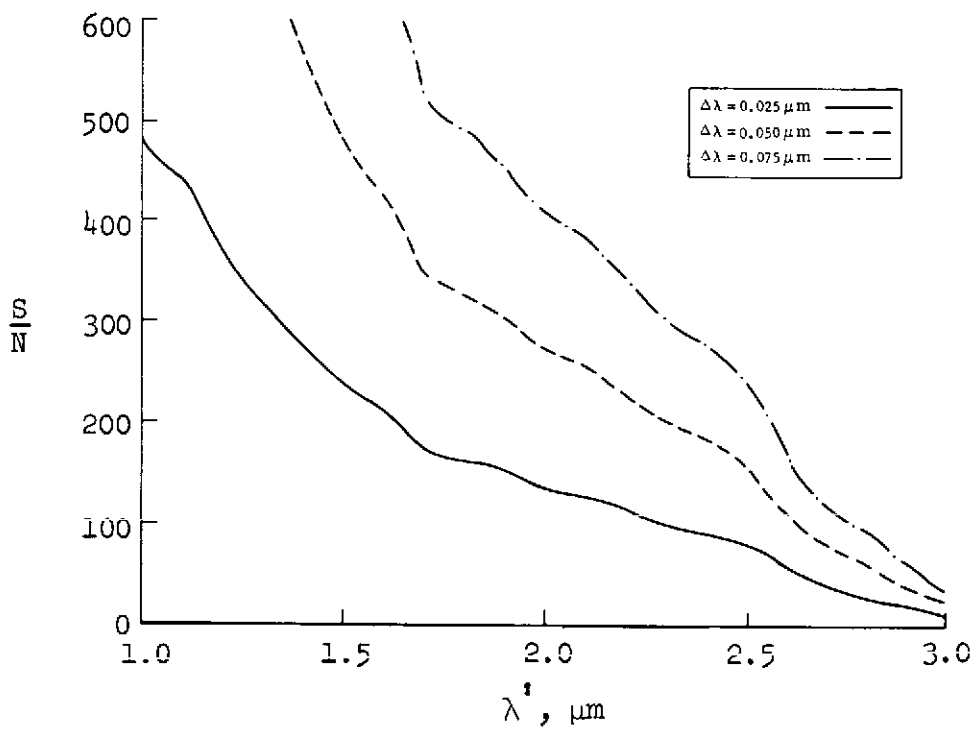
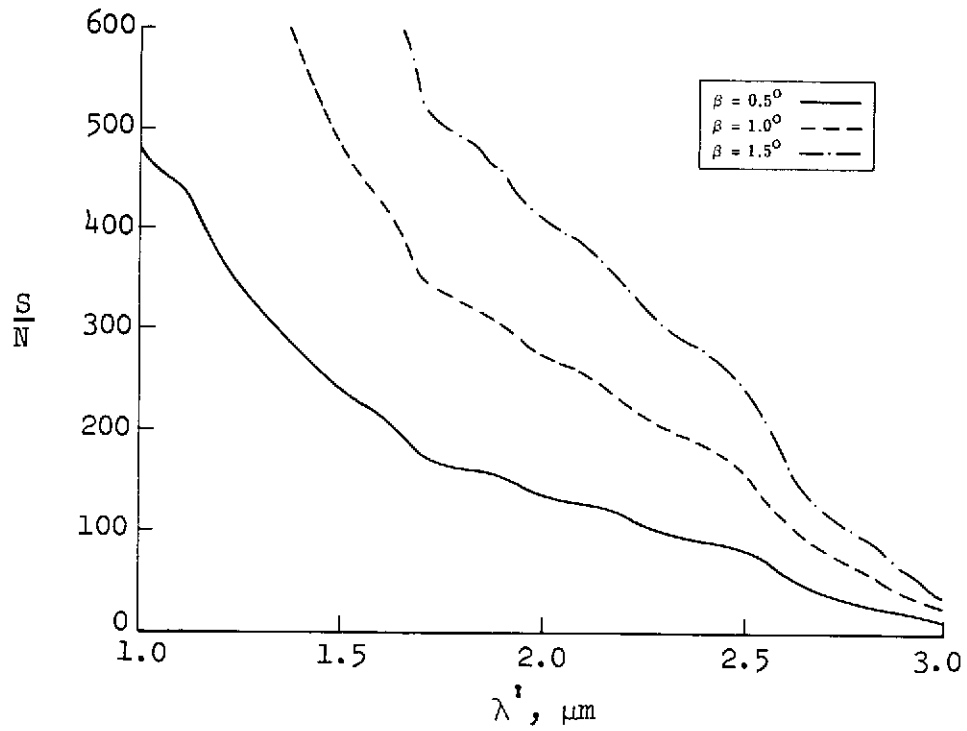
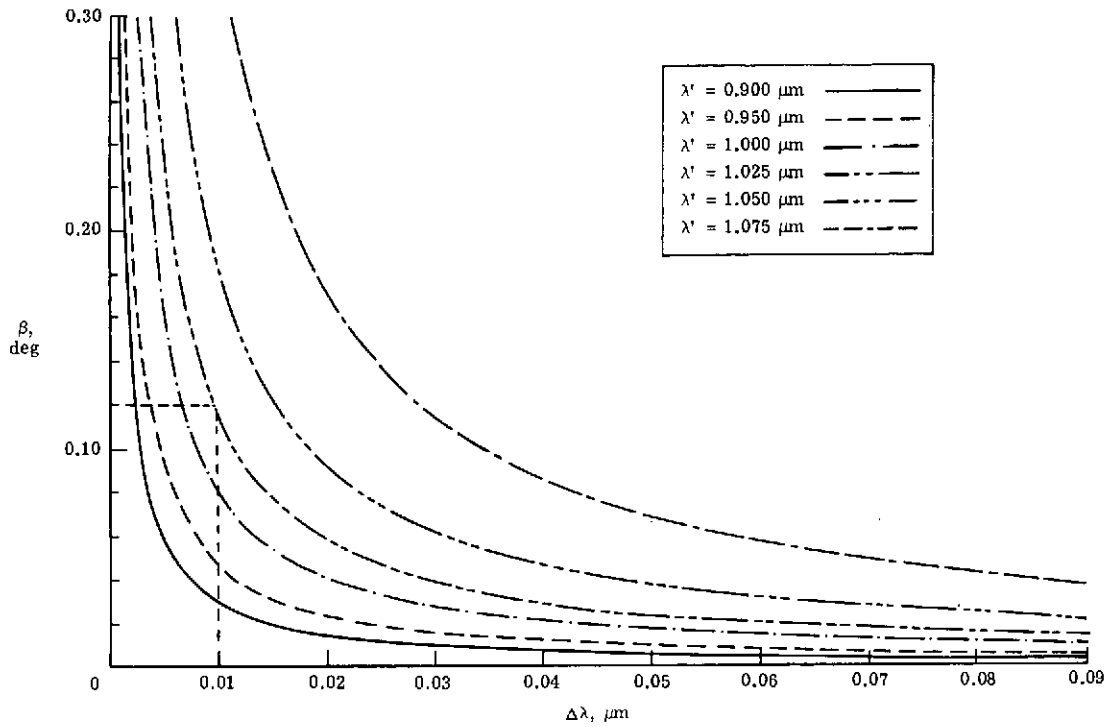
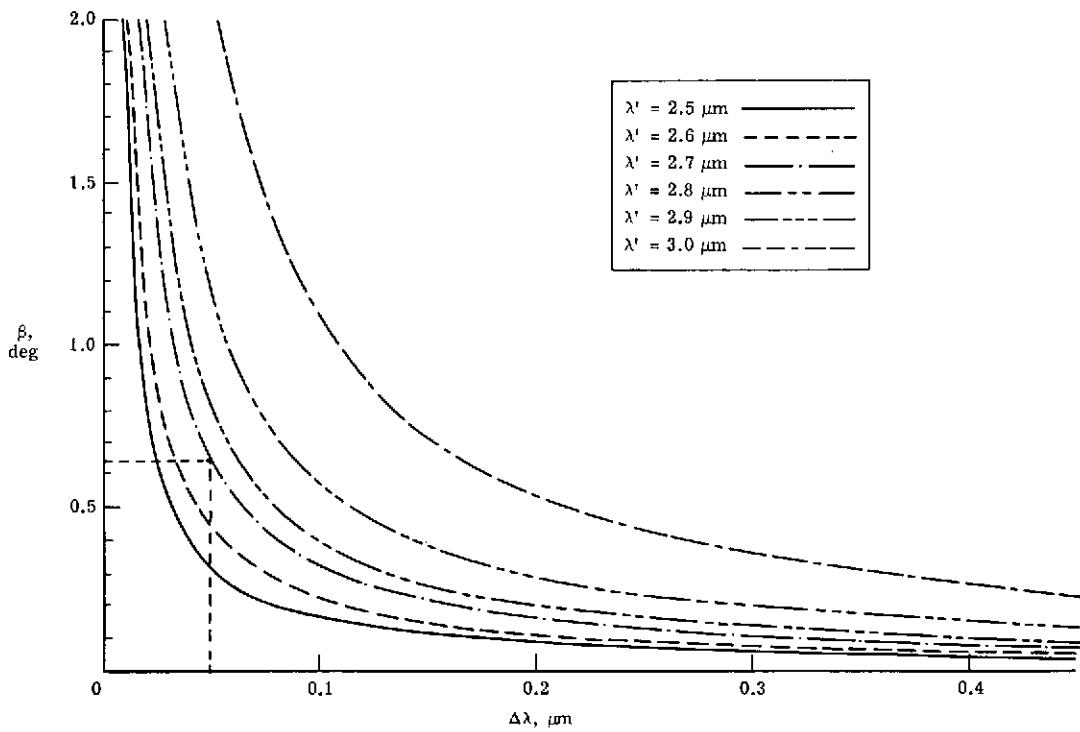


Figure 8.- Ratio of signal to rms noise for lead sulfide photodetector as a function of the filter center wavelength for constant (a) spectral resolution and (b) instantaneous field of view.

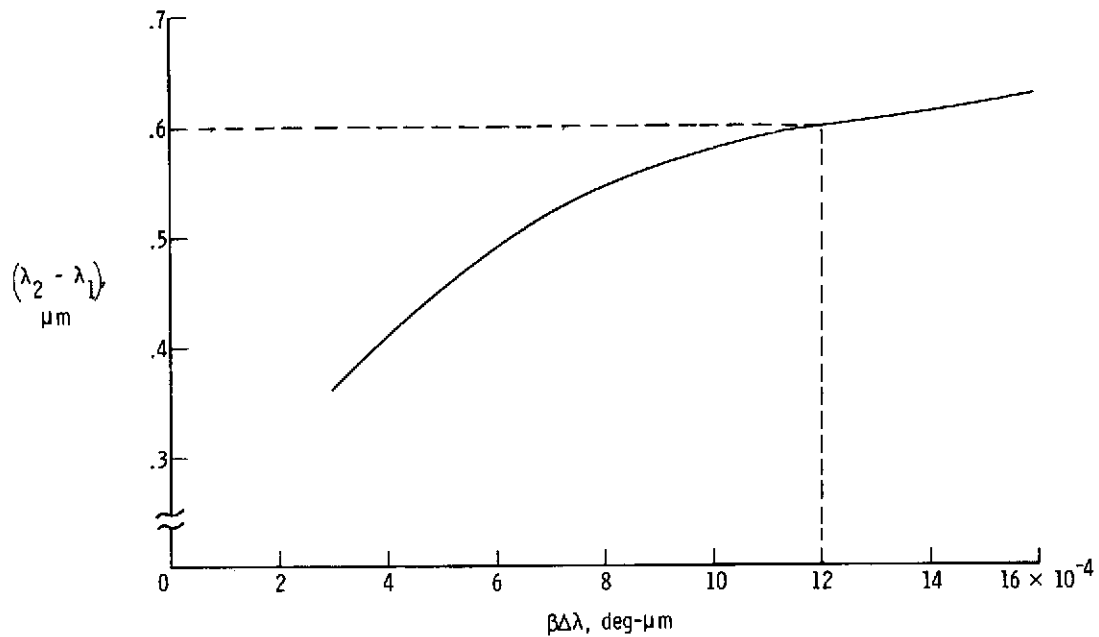


(a) Silicon.

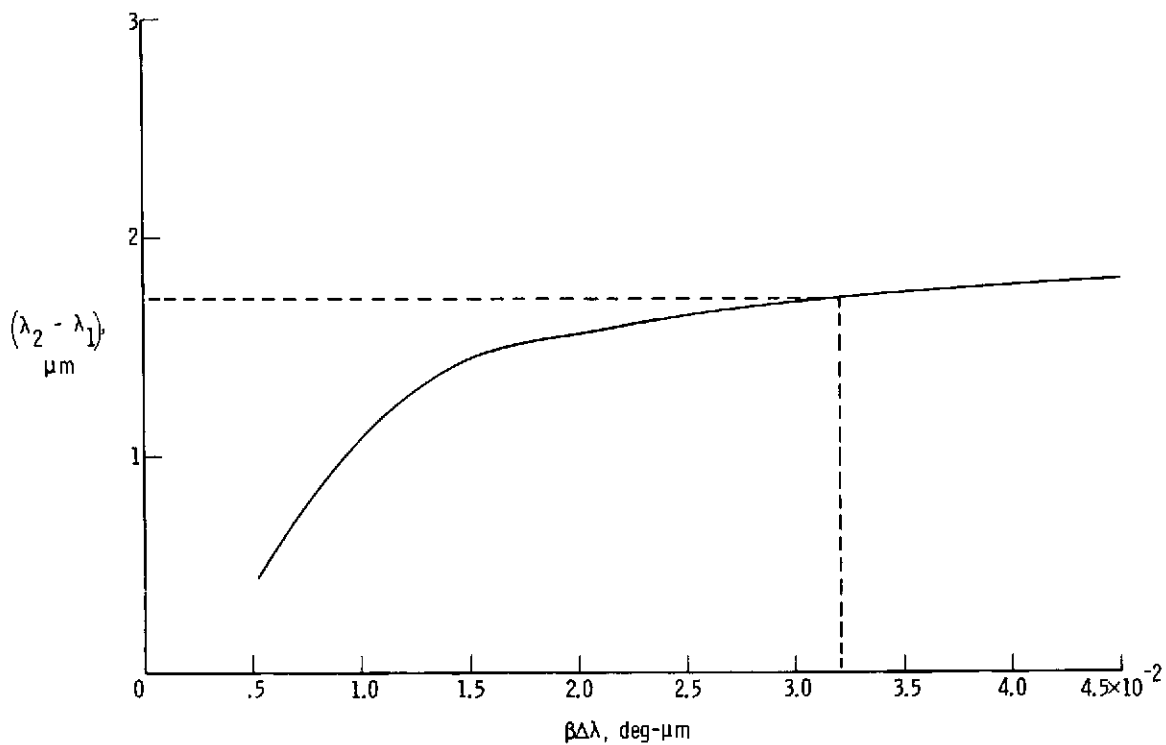


(b) Lead sulfide.

Figure 9.- Instantaneous field of view as a function of the filter spectral bandwidth for $\frac{S}{N} = 256$ at various upper limits of spectral range.

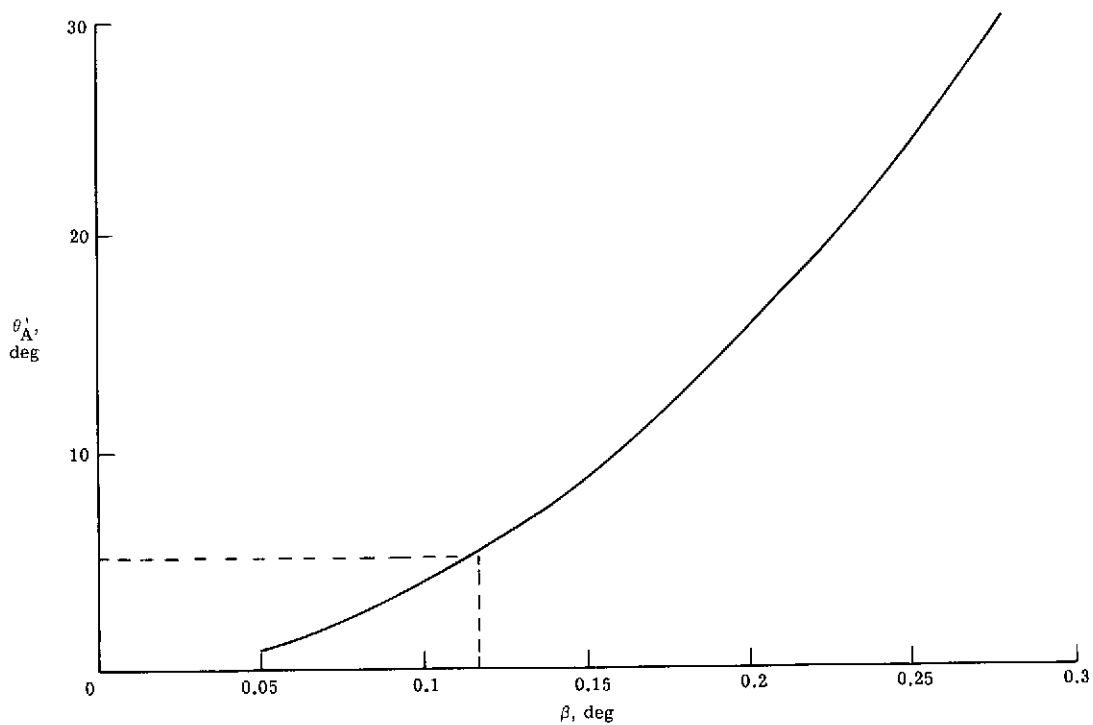


(a) Silicon.

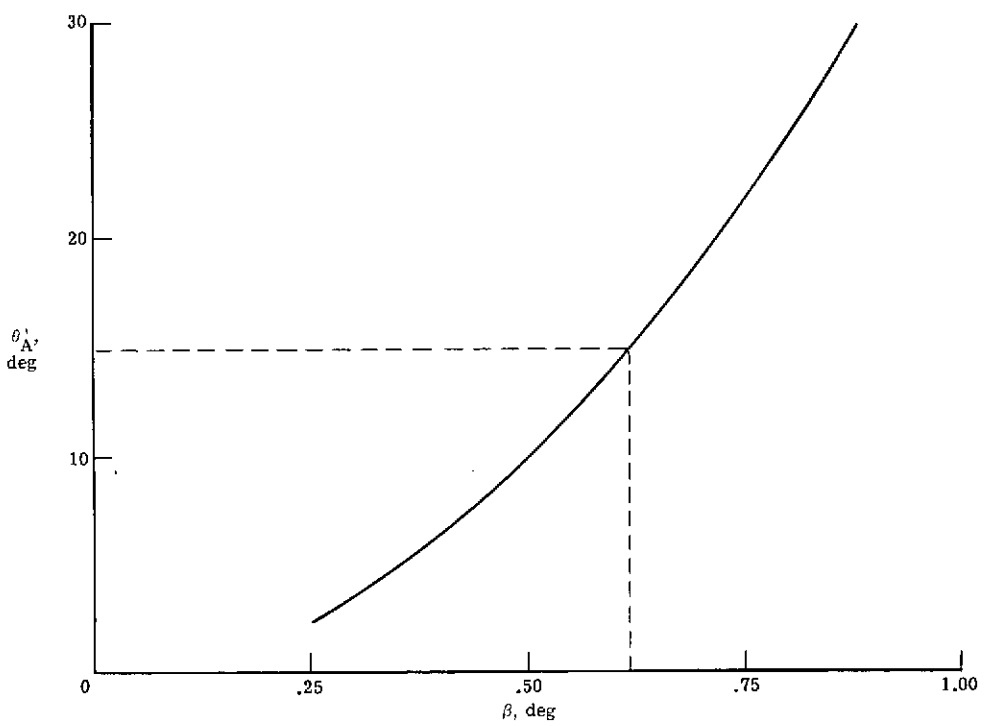


(b) Lead sulfide.

Figure 10.- Spectral range as a function of the product of instantaneous field of view and spectral resolution $\beta\Delta\lambda$ for $\frac{S}{N} \cong 256$.



(a) Silicon.



(b) Lead sulfide.

Figure 11.- Half-angle of image field required by photodetector array as a function of instantaneous field of view for $\frac{S}{N} = 256$.